Advances in Natural Sciences:
Nanoscience and Nanotechnology

Measurement and modelization of silica opal optical properties

OPEN ACCESS
IOP Publishing | Vietnam Academy of Science and Technology
Advances in Natural Sciences: Nanoscience and Nanotechnology
Adv. Nat. Sci.: Nanosci. Nanotechnol. **5** (2014) 015005 (6pp)
doi:10.1088/2043-6262/5/1/015005

Measurement and modelization of silica opal optical properties

Amaury Avoine[1,2], Phan Ngoc Hong[1,2,3], Hugo Frederich[1,2], Kifle Aregahegn[1,2], Paul Bénalloul[1,2], Laurent Coolen[1,2], Catherine Schwob[1,2], Pham Thu Nga[3], Bruno Gallas[1,2] and Agnès Maître[1,2]

[1] Sorbonne Universités, UPMC Univ. Paris 06, UMR 7588, Institut des NanoSciences de Paris, F-75005, Paris, France
[2] CNRS, UMR 7588, Institut des NanoSciences de Paris, Paris F-75005, Paris, France
[3] Institute of Materials Science, Vietnam Academy of Science and Technology, 18 Hoang Quoc Viet Road, Cau Giay District, Hanoi, Vietnam

E-mail: schwob@insp.jussieu.fr

Received 6 September 2013, revised 14 November 2013
Accepted for publication 3 December 2013
Published 30 December 2013

Abstract
We present the synthesis process and optical characterization of artificial silica opals. The specular reflection spectra are analyzed and compared to band structure calculations and finite difference time domain (FDTD) simulations. The silica optical index is a key parameter to correctly describe an opal and is usually not known and treated as a free parameter. Here we propose a method to infer the silica index, as well as the silica spheres diameter, from the reflection spectra and we validate it by comparison with two independent infrared methods for the index and, scanning electron microscopy (SEM) and atomic force microscopy (AFM) measurements for the spheres diameter.

Keywords: photonic crystal, optical characterization, specular reflection spectroscopy, effective index, band structure, FDTD simulations
Classification numbers: 5.04, 5.05

1. Introduction

Artificial opals are stackings of sub-micrometer dielectric spheres ordered in a compact crystallographic structure. They can be synthetized by various protocols of self-organization [1, 2]. They provide versatile and cost-efficient three-dimensional photonic crystals, and thereby present bands of forbidden light propagation [1, 3]. In the case of direct opals, the photonic band gaps are incomplete: the corresponding stop bands can be evidenced as peaks in the optical reflection spectra [4–11].

The dependence of the wavelength of these stop bands as a function of the considered propagation direction can be treated in two ways. A first way is to calculate numerically the three-dimensionnal band structure of the opal [12]. A second way is to model the opal by a lattice of scattering points (located at the center of the spheres) in a homogeneous medium with an effective index n_{eff}. At a given incident light angle, the opal stop band wavelength is then provided by Bragg's law, which expresses the condition for constructive interferences between beams reflected by parallel planes of scattering points [4, 5, 13–15]. The underlying question is whether the opal can be described as a homogeneous medium, although the size of the spheres is of the same order as the considered wavelength.

A fine quantitative comparison between the models and the experimental optical data is delicate because, whereas the spheres diameter can be measured by atomic force or electron microscopies, the silica optical index has not, to our knowledge, been measured independently and is always treated as a free parameter.

In this paper, we describe the methods used to synthetize silica spheres and opals. Then we perform and analyze specular reflection spectra of silica opals. We demonstrate an original method to extract, from these optical data, the values of the silica index and of the spheres diameter. We validate this method by comparing its results to other independent

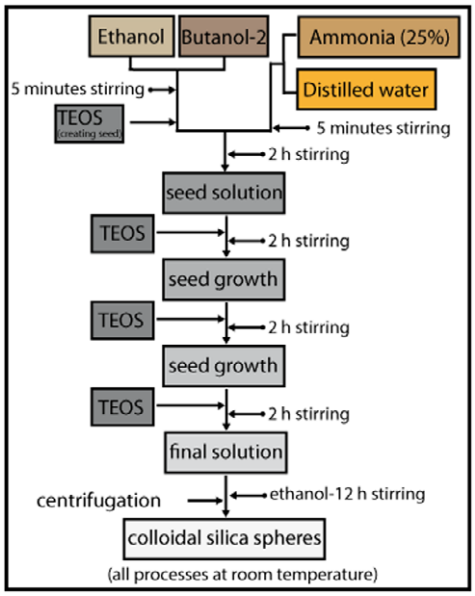

Figure 1. Process used to synthetize silica spheres.

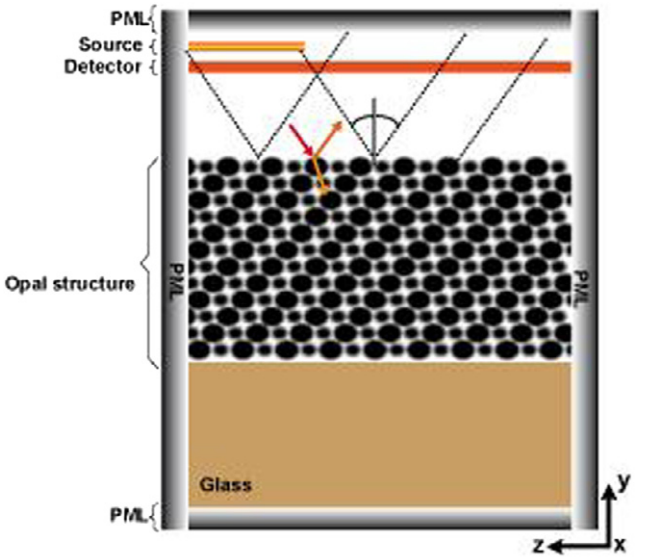

Figure 2. Representation of the computation cell used in FDTD calculations.

techniques. We calculate the band structure of our opals and simulate the reflection spectra for different angles, with the effective index and spheres diameter inferred from our optical method. Finally, we compare the obtained results to the experimental data and to Bragg calculations.

2. Experiments

2.1. Synthesis of silica spheres and opals

The opals were synthetized using the convection self-assembly protocol [16] from home-made silica spheres. These ones were obtained from a procedure derived from the Stober method [17]. The key point to fabricate high crystallographic quality opals over large monodomains is the low size dispersion of the spheres. For this purpose, we used a 'multi-steps' synthesis protocol in which the silica precursor is added first in one drop to create silica seeds, and then by steps to grow the seeds.

The procedure is described in figure 1. First, a mixture of alcohols (80 ml of ethanol and 20 ml of butanol-2) was stirred for 5 min at room temperature. Then, 3 ml of tetraethyl orthosilicate (TEOS) was added, as quickly as possible, with 5 min stirring to ensure homogeneity. Next, 7 ml of ammonia and 8 ml of deionized water were added drop by drop in the vessel. After 120 min, the synthesized silica seeds have reached their final size.

Then, 3.2 ml of TEOS was added slowly in the colloidal seeds solution under continuous rotation of the magnetic stirrer. The rate of addition of the TEOS solution, equal to 8 ml h^{-1}, was controlled precisely by using an automatic syringe. After the 3.2 ml of TEOS was dropped, the solution was kept for 2 h in the same conditions before adding another 3.2 ml of TEOS. This process could be repeated several times (three times in our case) in order to increase the diameter of particles. Moreover, this process allows one to obtain very low size dispersion, on the order of 3.5%. Then, 70 ml of ethanol were added into the solution. After 12 h, the magnetic stirrer was stopped. The obtained silica spheres were finally selected in size and cleaned in ethanol using a centrifugation machine. They were dried in a heater at 60 °C overnight to weigh the residual solid. A certain amount of these silica spheres was then dissolved in a certain amount of pure ethanol in order to have the required concentration. Before performing the opal synthesis, this colloidal solution was put in an ultrasonic bath for at least 6 h to disperse the spheres in ethanol.

The experimental set up to synthetize opals corresponds to the one commonly used in convection protocols. The synthesis of opal took place in a cylinder beaker of 25 ml with diameter of 35 mm. A microslide was held in a slot designed in a teflon rectangular parallelepiped. This slot allowed tilting the substrate with respect to the vertical direction with a 30° angle. A temperature gradient between the top and the bottom of the beaker was created. The upper part was at room temperature (25 °C), while the temperature of the bottom part could vary thanks to a heater (resistor controlled temperature (RCT) basic safety control, IKA). Thanks to an external PT1000 temperature sensor fixed at the bottom of the beaker, the heater could heat and maintain a temperature at the set point (40 °C for the sample presented here) with an accuracy of 1 °C.

Then, 25 ml of 10 wt% silica alcosol was introduced gradually by a plastic pipette. All experimental steps were done under an extractor hood in a low-vibration environment.

2.2. Specular reflection spectra

The opal specular reflection spectra were measured at various incidence angles.

The incidence beam was provided by a halogen lamp connected to an optical fiber (core 600 μm), mounted on a goniometer arm with a collimator (focal length 12.7 mm) and a diaphragm (diameter 0.6 mm). The reflected beam was collected by a symmetric collimated fiber (with 1 mm diaphragm) and analyzed by a spectrometer (resolution 1.5 nm). The overall goniometer resolution was 1°. All the spectra were normalized by the incident light spectrum.

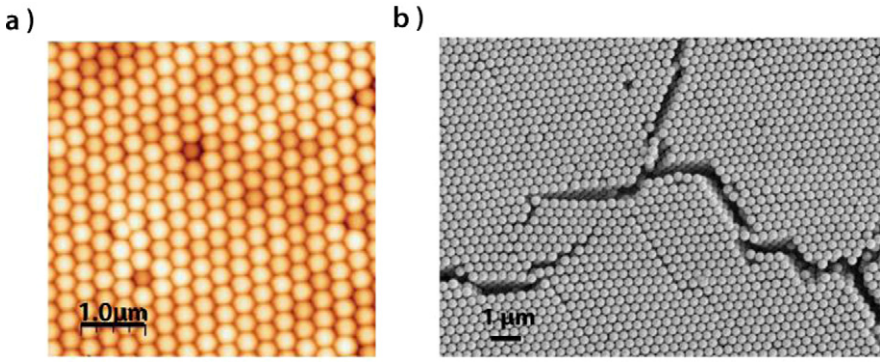

Figure 3. (a) AFM and (b) SEM images of the upper surface of a silica opal obtained by convection protocol.

2.3. Finite difference time domain (FDTD) calculations

The experimental reflection spectra were compared with FDTD simulations using MEEP (an acronym for MIT electromagnetic equation propagation) tool [18]. This method consists in calculating the propagation of the electromagnetic field from a given light source through a computed structure from the Maxwell equations. For this, space and time are divided into a regular grid. The basic mechanism of this method is to discretize Maxwell's equations and to solve them in the leapfrog manner: the electric field vector components in a volume of space are solved at a given in time; then the magnetic field vector components in the same spatial volume are solved at a given time further; and the process is repeated until the desired transient or steady-state electromagnetic field behavior is fully evolved.

The computation cell is presented in figure 2.

The opal, composed of nine layers (in y direction) of silica spheres (diameter 331 nm and index 1.39) in a fcc structure, is placed on a glass substrate. It is shone on by a light source of fixed frequency. The size of the source (in the xOz plane) is chosen to be equal to 2 μm (six spheres) to avoid scattering and it is located at 900 nm from the closest layer of the opal. To perform reflection spectra at non-normal incidence, the wavevector is tilted by a certain angle in the xz-direction by introducing a $2\pi k_z z$ phase in the source. A detector, having the same dimensions as the cell in the (xOz) plane and dimensionless in y-direction, is located between the source and the opal at 800 nm from the first opal layer. It is obviously too close to ensure far-field detection, but an enhancement of the distance would have led to an enhancement of the size of the cell and so of the memory and time needed to perform the simulation. Note that the detector does not affect the propagation of the incident light to the opal. Absorbing perfectly matched layers (PMLs) are placed all round the cell in the three dimensions to avoid reflections. Each run gives the flux corresponding to a single excitation wavelength. So to obtain the whole spectrum, from 500 to 750 nm by steps of 5 nm, at a given angle, 7 days of computation are needed with our computing power (processor 2.93 GHz, 4Mo). The incident flux is measured by running the simulation without the opal. In the presence of opal, the incident flux (which is also measured) is substracted from the total flux to obtain the reflected one, and is used to normalize the spectra.

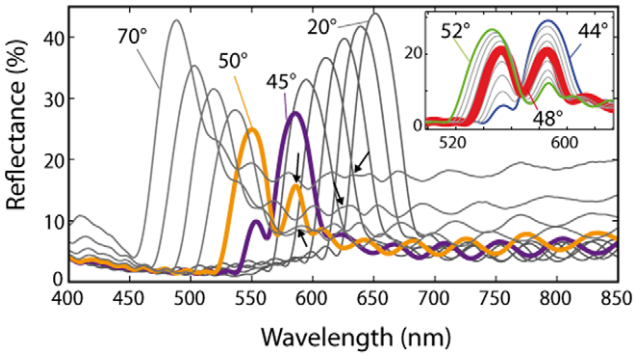

Figure 4. Unpolarized reflection spectra of the opal sample for incidence/reflection angles θ ranging from 20° to 70° by steps of 5°. The secondary peak is indicated by arrows. (inset) Unpolarized reflection spectra for θ from 44° to 52° by steps of 1°.

3. Results and discussion

3.1. Synthesis of silica spheres and opals

Figure 3 shows atomic force microscopy (AFM) and scanning electron microscopy (SEM) images of the opals obtained by convective method from the homemade silica spheres. In spite of some line defects over scales of tenths of microns, these images evidence a well-ordered compact structure and a preserved lattice orientation. The spheres diameter inferred from measurements on these images of the surface periodicity is equal to 330 ± 10 nm.

3.2. Effective index and spheres diameter determination

Figure 4 displays the measured unpolarized reflection spectra. For all specular angles θ, we observe a main reflection peak which is blue-shifted from 650 to 490 nm as θ increases. For θ larger than 40°, a secondary peak, indicated by arrows in figure 4, appears: this peak is red-shifted as θ increases. For $\theta = 48°$ an avoided crossing (as will be evidenced on the band diagram) where the two peaks have the same height, is observed (see inset of figure 4). The minor amplitude oscillations at higher wavelengths correspond to Fabry–Perot interferences between the air/opal and opal/substrate interfaces.

In the following, we present an original method, based on the avoided crossing interpretation, to infer the silica optical index from the reflection spectra.

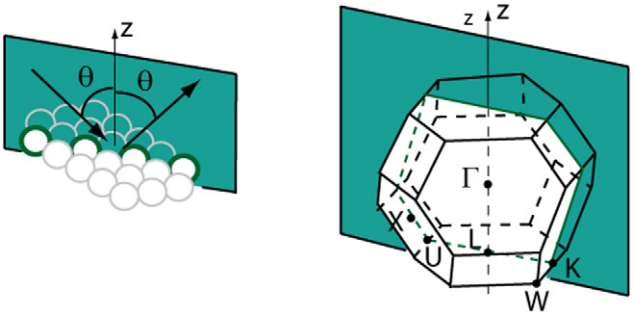

Figure 5. Schematic of the chosen experimental incidence plane (in green), in the real space (left) and in the opal first Brillouin zone (right).

The first Brillouin zone of the opal face-centered-cubic (fcc) lattice, with its high-symmetry points X, U, L, K and W, is represented in figure 5. The experimental vertical z-direction, normal to the (111) opal plane, corresponds to the (ΓL) line in the **k** space. The incident and reflected beams, corresponding to the experimental reflection spectra, are in the XUK plane, indicated by green planes in figure 5.

Band structure calculations, developed in the last section, confirm the observations made on specular reflection spectra (see figure 7). Indeed, for θ-angle between 20° and 80°, two stopbands, with an avoided crossing when the wavevector **k** reaches $\Gamma\mathbf{K}$, are evidenced. For this given direction, the internal propagation angle θ_{int} (relative to the vertical direction (ΓL)) is

$$\theta_{\text{int}} = \sin^{-1}\frac{1}{\sqrt{3}} = 35.3^{\circ}.$$

If we consider that the two experimental peaks anticross at the K point, the value of the external angle $\theta = \theta_K$ can be inferred, with a 1° precision, from the reflection spectra by measuring the θ value for which the two peaks have the same height. Thus, by assuming the validity of the Snell's law in the opal medium ($\sin\theta = n_{\text{eff}}\sin\theta_{\text{int}}$), the opal effective index n_{eff} is given by

$$n_{\text{eff}} = \sqrt{3}\sin\theta_K. \qquad (1)$$

The silica index n_{sil} is related to n_{eff} by the Bruggeman effective medium approximation [19]

$$f\frac{n_{\text{sil}}^2 - n_{\text{eff}}^2}{n_{\text{sil}}^2 + 2n_{\text{eff}}^2} + (1-f)\frac{1-n_{\text{eff}}^2}{1+2n_{\text{eff}}^2} = 0, \qquad (2)$$

where f is the filling factor ($f = 0.74$ with the hypothesis that the opal presents a compact lattice).

Moreover, we can extract the silica spheres diameter D by measuring, at incidence angle θ_K, the value of the wavelength λ_K corresponding to the middle value of the maximum wavelengths of the two reflection peaks. The theoretical angular frequency ω of the avoided crossing is close to its value in the homogeneous-medium approximation

$$\omega = \frac{c\,\|\mathbf{k}\|}{n_{\text{eff}}} = \frac{c\,\|\Gamma\mathbf{K}\|}{n_{\text{eff}}} = 3\pi\frac{c}{2Dn_{\text{eff}}},$$

so with

$$\lambda = \frac{2\pi c}{\omega},$$

Table 1. Parameters D (spheres diameter), n_{eff} (opal effective index) and n_{sil} (silica beads index) obtained for the opal shown in figure 3 by AFM, SEM, infrared ellipsometry, infrared spectroscopy, visible reflection spectra (method introduced in this section) and fit by Bragg's law.

Method		Value
SEM and AFM images	D (nm)	330 ± 10
IR ellipsometry	n_{eff} (deduced from n_{sil})	1.29
	n_{sil} (measured)	1.39
IR spectroscopy	n_{eff} (deduced from n_{sil})	1.29
	n_{sil} (measured)	1.39
Reflection spectra		
Equation (1)	n_{eff} (measured)	1.29 ± 0.02
Equation (2)	n_{sil} (deduced from n_{eff})	1.39 ± 0.02
Equation (3)	D (nm)	331
Bragg fit (equation (4))	n_{eff} (measured)	1.37
	n_{sil} (deduced from n_{eff})	1.51
	D (nm)	301

we obtain the silica spheres diameter

$$D = \frac{3\lambda_K}{4n_{\text{eff}}}. \qquad (3)$$

In order to validate this method, we compared the obtained silica index and spheres diameter with two independent index measurements, based on infrared ellipsometry and spectroscopy (photon lines) [20], and with SEM and AFM measurements for the diameter D (see table 1). Finally, we compared the obtained values with the ones inferred from the Bragg's law for interferences between diffractions on the (111) planes:

$$\lambda_{\max} = 2\sqrt{\frac{2}{3}}D\sqrt{n_{\text{eff}}^2 - \sin^2\theta}, \qquad (4)$$

using n_{eff} and D as fitting parameters to adjust the theoretical expression on the values $\lambda_{\max}$ corresponding to the main peaks maxima of the experimental reflection spectra.

The results summarized in table 1 show the good agreement between the method we developed to extract the opal effective index and the spheres diameter from the reflection spectra and other independent methods (IR ellipsometry and spectroscopy for the index, SEM and AFM measurements for the diameter). Conversely, the Bragg-fitted values of n_{eff} and D, presented in table 1, are quite far from the other ones, demonstrating the limitations of the Bragg one-dimensional modelization.

3.3. FDTD simulations

We performed FDTD simulations on reflection spectra at 20°, 30° and 40° specular angles. A satisfying agreement is obtained between the simulated and experimental positions of the reflection maxima (see table 2).

3.4. Band structure calculations

For our experimental geometry, the band gap can be reached when **k** crosses (LK) (figure 6). We thus calculate, using a freely available software [21], the band structure for **k** along this line, with the values of n_{eff} and D extracted from the reflection spectra, in order to determine the opal stopbands.

Table 2. Values of maxima wavelengths from experimental reflection spectra and FDTD calculations for different angles.

Angle (°)	λ_{max} experiment (nm)	λ_{max} simulation (nm)
20	652	667
30	627	642
40	596	612

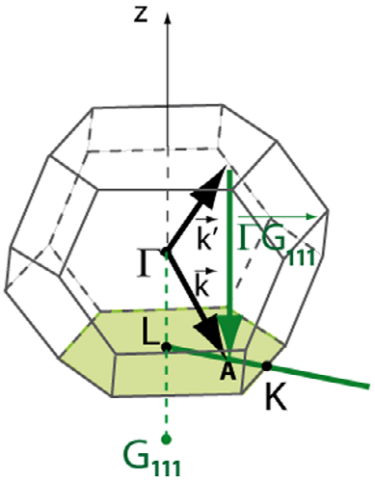

Figure 6. Schematic of Laue's geometric condition for diffraction by the (111) planes.

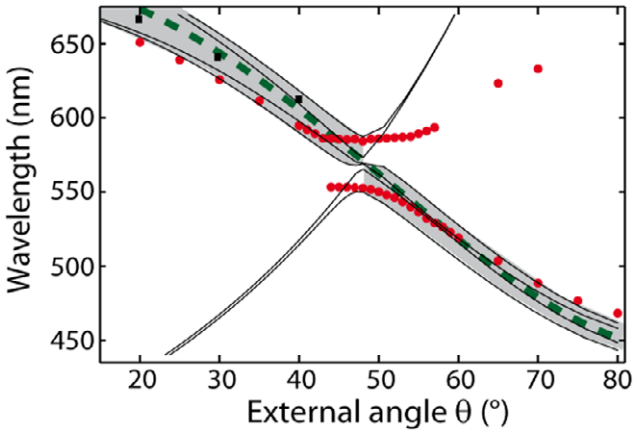

Figure 7. Experimental reflection peaks positions $\lambda(\theta)$ (red circles) superimposed on the band structure for **k** along the (*LK*) line (111 planes) (full lines), on Bragg's equation (dotted green line) and on FDTD calculations (black squares) . Band structure, Bragg equation and FDTD calculations were calculated with the values $n_{sil} = 1.39$ and $D = 331$ nm extracted from the reflection spectra of figure 4 as explained above. The stop bands are shaded in gray.

In figure 7, we plot the band structure along the (*LK*) line together with the experimental and simulated peak positions λ_{max} for different values of the specular angle θ. We find a good agreement between band structure calculations, and simulated and experimental peak positions. We also plot the (111) Bragg equation in dotted lines, with the D and n_{eff} values extracted from the reflection spectra. It matches very well the simulated peaks positions and the calculated band structure and satisfyingly the experimental data. A better agreement between Bragg's law and the main peak positions can be obtained by adjusting the parameters n_{eff} and D. However, the fitted values (given in table 1) are, for the opal considered in the present work, far from the actual values obtained by AFM, SEM, infrared ellipsometry and spectroscopy.

4. Conclusion

In this paper, we presented the synthesis of silica spheres and silica opals and analyzed the specular reflection spectra of the obtained opals. By relating the avoided crossing of the two peaks observed on the spectra with the K point of the Brillouin zone, we established an original method to extract the opal effective index and the diameter of the silica spheres. We validated this method by comparing these results with values of index and spheres diameter provided by other independent techniques. We showed a good agreement between band structure calculations and experimental and simulated determinations of the reflection maxima spectral positions.

Acknowledgments

The authors thank Eric Charron and Willy Daney de Marcillac (INSP) for their work on the goniometer setup, Emmanuelle Lacaze and Dominique Demaille (INSP) for their help, respectively, on AFM and SEM measurements, Pierre-Richard Dahoo and Jean-Maurice Coanga (Université de Versailles—Saint-Quentin en Yvelines) for their help on infrared measurements, and Carlos Barthou (INSP) for its fruitful advice. The collaboration between INSP and IMS was supported by a Projet International de Coopération Scientifique (PICS 5724) between CNRS and VAST. Pham Thu Nga would like to thank the Vietnam National Foundation for Science and Technology Development (NAFOSTED) for supporting her under grant no. 103.06-2011.03.

References

[1] Lopez C 2003 *Adv. Mater.* **15** 1679
[2] Marlow F, Muldarisnur M, Sharifi P, Brinkmann R and Mendive C 2009 *Angew. Chem. Int. Edn* **48** 6212
[3] Tarhan I I and Watson G H 1996 *Phys. Rev. Lett.* **76** 315
[4] Baryshev A V, Khanikaev A B, Fujikawa R, Uchida H and Inoue M 2007 *Phys. Rev.* B **76** 014305
[5] Moroz A V, Limonov M F, Rybin M V and Samusev K B 2011 *Phys. Sol. State* **53** 1105
[6] van Driel H M and Vos W L 2000 *Phys. Rev.* B **62** 9872
[7] Galisteo-Lopez J F, Lopez-Tejeira F, Rubio S, Lopez C and Sanchez-Dehesa J 2003 *Appl. Phys. Lett.* **82** 4068
[8] Baryshev A V, Kaplyanskii A A, Kosobukin V A, Limonov M F and Skvortsov A P 2004 *Phys. Solid State* **46** 1331
[9] Bazhenova A G, Sel'kin A V, Men'shikova A Yu and Shevchenko N N 2007 *Phys. Solid State* **49** 2109
[10] Vion C, Barthou C, Bénalloul P, Schwob C, Coolen L, Gruzintev A, Emel'chenko G, Masalov W, Frigerio J-M and Maître A 2009 *J. Appl. Phys.* **105** 113120
[11] Nair R V and Jagatap B N 2012 *Phys. Rev.* A **85** 013829
[12] Lopez-Tejeira F, Ochiai T, Sakoda K and Sanchez-Dehesa J 2002 *Phys. Rev.* B **65** 195110
[13] Baryshev A V, Kaplyanskii A A, Kosobukin V A, Limonov M F, Samusev K B and Usvyat D E 2003 *Phys. Solid State* **45** 459

[14] Romanov S G, Maka T, Sotomayor Torres C M, Müller M, Zentel R, Cassagne D, Manzanares-Martinez J and Jouanin C 2001 *Phys. Rev.* E **63** 056603
[15] Tikhonov A, Bohn J and Asher S A 2009 *Phys. Rev.* B **80** 235125
[16] Jiang P, Bertone J F, Hwang K S and Colvin V L 1999 *Chem. Mater.* **11** 2132
[17] Stöber W, Fink A and Bohn E 1968 *J. Colloid Interface Sci.* **69** 62
[18] Oskooi A F, Roundy D, Ibanescu M, Bermel P, Joannopoulos J D and Johnson S G 2010 *Comput. Phys. Commun.* **181** 687
[19] Egan W G and Aspenes D E 1982 *Phys. Rev.* B **26** 5313
[20] Avoine A, Hong P, Frederich H, Frigerio J-M, Coolen L, Schwob C, Nga P, Gallas B and Maître A 2012 *Phys. Rev.* B **86** 165432
[21] Johnson S G and Joannopoulos J D 2001 *Opt. Express* **8** 173